

THz RADIATOR BASED ON PHOTONIC BAND GAP CRYSTAL FOR SwissFEL*

L. Shi[†], S. Reiche, R. Ischebeck, Paul Scherrer Institut, CH-5232 Villigen PSI, Switzerland

Abstract

The electromagnetic radiation in 1–20 THz has many unique properties when it interacts with matter due to its non-ionizing excitation in matter. Especially the dynamics of the excited matter can be probed with the help of X-ray pulses at a free electron laser facility, e.g., SwissFEL, to deepen our understanding of a wide range of phenomena. Due to its high research potential, various means of THz generation have been proposed and demonstrated. We investigate preliminarily here its generation based on a relativistic electron bunch and a photonic band gap crystal (PBG) made of dielectric rods. The PBG provides additional degrees of freedom for the THz pulse tuning. Additionally, the unwanted radiation parts can be damped by the structure in order to minimize the deleterious beam dynamics effects. The crystal also promises the integration of generation, filtering and coupling for transport into a single piece.

INTRODUCTION

The electromagnetic radiation in 1–20 THz has many spectroscopic properties when it interacts with matter. In particular the non-ionizing excitation of phonons in matter, which is important to understand the physiochemical as well as biological processes of condensed matter [1]. The dynamics of the matter then can be probed with X-ray pulses at a free electron laser facility [2]. The generation of THz can be based on optical rectification for a broadband [3], quantum cascaded lasers, dedicated accelerator beam lines etc. [4]. The narrowband THz pulses find their places in a range of matter excitation researches [5]. The generation of narrowband, high power THz pulses have been exemplified in several labs based on the dielectric lined waveguides [6–8]. However, the circular dielectric lined waveguide (DLW) limits the tunability to its supported modes once the geometry is fixed. The tuning can only be achieved by changing the electron beam [7, 9]. Inspired by the DLW and the work from photonic band gap crystal (PBG), we here investigate the feasibility of generating tunable narrowband THz pulses with the PBG. The prerequisite of the electron beam for the excitation is readily available from our free electron laser, SwissFEL [10].

A photonic band gap structure [11] for photons works in a similar way as the band gap of a semiconductor for electrons in solid state physics. Several pioneer investigations have been carried out to study its electrical properties in radio frequency range for acceleration purposes and the mitigation of the transverse wake fields has been demonstrated experimentally [12–15]. For acceleration operation, the geometry

of the structure is preferably fixed in order to provide stable acceleration. For the radiation generation, the structure is better to be tunable mechanically and thus the generated radiation is able to accommodate various experimental needs. We also noticed the tunability of the dielectric material via, say Kerr effect, but it is not discussed at this stage.

The photonic band gap crystals represent a family of crystals and therefore it is impossible to discuss them exhaustively here. We start our photonic band gap structure design from a waveguide with the analogy from a dielectric lined waveguide with circular cross section, which provides the highest coupling between the electron beam and the waveguide. We first discuss a possible design of the band gap structure and compare it with its counterpart waveguide whenever appropriate. The potential means of tuning are followed. We also actively prepare the necessary experimental infrastructure for such an experiment. A brief introduction to our experimental platform—the vacuum chamber for accelerator on a chip program (ACHIP) [16] is given before we conclude the paper.

PHOTONIC BAND GAP WAVEGUIDE

In order to efficiently generate radiation, several conditions should be met: the mode (electromagnetic field distribution) should be confined and exhibit electric field along the beam movement direction; the phase velocity of the mode, normally transverse magnetic mode with azimuth symmetry, should be synchronized with the electron beam [17]. For the mode transverse confinement, it is either from the metallic coating, as in a dielectric lined waveguide or some band gap from the photonic structures as shown in Fig. 1.

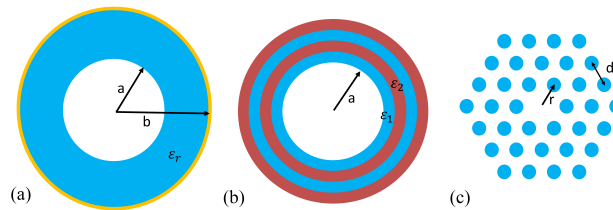


Figure 1: Transverse cross section of (a) a dielectric lined waveguide, (b) a Bragg fiber, and (c) dielectric rod waveguide. (For conceptual illustration only.)

The DLW (Fig. 1-a) consists of a vacuum passage for the electron beam movement surrounded by a layer of dielectric material ϵ_r with a metallic coating (yellow part) for the mode confinement. The Bragg fiber (Fig. 1-b) has multiple layers of alternating dielectric material to provide destructive reflections (to form a band gap) so that a mode of a certain frequency in the gap is confined and the others can leave the region. The alternative layers are in analogy to the metallic

* Work supported by Marie Curie Action H2020

[†] liangliang.shi@psi.ch

layer in a hollow metallic waveguide [18]. The equivalent DLW certainly can be realized as well. But Figs. 1-a and c seem difficult to couple to a mechanical tunability to achieve a different family of modes. Replacing the continuous layers of dielectric material with discrete dielectric rods leads to the design of a waveguide of similar functionality based on dielectric rods in Fig. 1-c. This provides the extra degrees of freedom for various mechanical couplings.

In Fig. 1, the electron beam moves perpendicular to paper along the rotation symmetry axis \mathbf{z} and the structure is assumed to be infinitely long for the ease of discussion. The electromagnetic field distribution can be written in the Bloch state [11],

$$\mathbf{H}_{(n,k_z,\mathbf{k}_\parallel)}(\mathbf{r}) = e^{i\mathbf{k}_\parallel \cdot \rho} e^{ik_z z} \mathbf{u}_{(n,k_z,\mathbf{k}_\parallel)}(\rho) \quad (1)$$

where \mathbf{k}_\parallel and k_z are the wave vectors in the transverse and longitudinal direction, respectively. The field distribution in a periodic unit is $\mathbf{u}_{(n,k_z,\mathbf{k}_\parallel)}$. We here consider the mode polarized in z direction with azimuth symmetry and they are referred to be as monopole TM modes. From the symmetry point of view [11], k_z is preserved due to the translational symmetry, which can be used for mode guiding. \mathbf{k}_\parallel is conserved only at discrete values and produces band gaps so that for certain $(\mathbf{k}_\parallel, k_z)$, the mode can only be guided along k_z .

The band structure of a triangular lattice (Fig. 1 with a central rod) is calculated with the software package MPB [19] and the definition of primitive Brillouin zone is defined in appendix B of reference [11]. The dispersion curves are shown for both the TE (polarized in the transverse plane) and TM bands in Fig. 2.

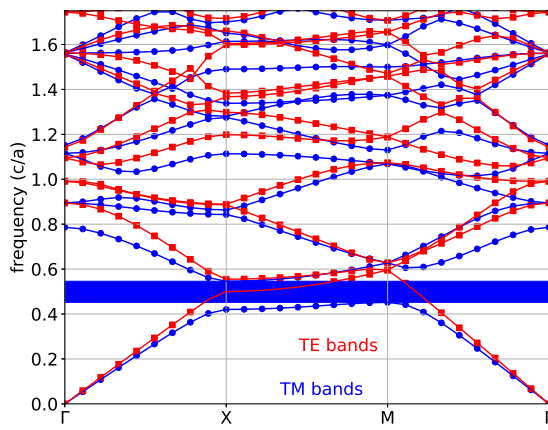


Figure 2: Band structure of triangular quartz rods based lattice for both TE and TM modes along the irreducible Brillouin zone as defined in [11].

There is no band gap for TE modes but there is a larger one for TM band. At higher frequencies, there are no band gaps because the corresponding wavelengths become shorter and the crystal is simply not effective for these length scales. The higher order modes are potentially damped, which can

be detrimental to the electron beam movement. We will focus on the first TM band gap. The lattice is made of quartz with $\epsilon_r = 3.8$. Parametric study shows that a higher permitivity favors a larger band gap, which generally shows better trapping of the mode (less leakage from side ways). The band gap is 0.45-0.54 with a relative gap of 18% (defined as the ratio between the mid-frequency and the gap) here, whereas the band gap is 0.27-0.45 with a relative gap of 47% for $\epsilon_r = 12$. Since the Maxwell equations are scale invariant, the only variable parameter is the rod radius. In Fig. 3, we show the dependence of the relative band gap on the rod radius.

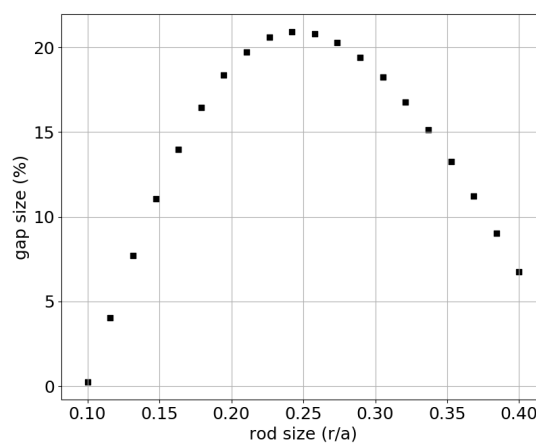


Figure 3: Band gap size versus rod size.

The optimized gap is at $r = 0.24a$ with the gap size 22%. If the rod radius is too small, the crystal is not effective and there is virtually no gap. On the contrary, the gap also disappears when the distance between rods becomes smaller. Obviously, when $r = 0.5a$ the rods start to contact each other forming a bridge and in this case the TM gap would disappear while a TE gap is expected.

Now we can remove a rod to form a defect in the crystal as in Fig. 1-c. Of course, we are free to remove more layers. The E_z of the three consecutive modes with the same wave vector is shown in Fig. 4. We indeed observe a monopole like mode that is trapped in the defect site. The mode frequency (0.46) is close to the mid frequency of the band gap and close to 50% of the mode energy is trapped in the defect site. For the other two modes, they present multi-modal distributions and can travel in the crystal.

Since we used the normalized units here, the interesting quantities can always be retrieved by scaling. For example, we wan to operate our crystal in 1 THz for the defect mode and crystal constant a is close to 138 μm with a rod radius of 33 μm .

We have shown essentially that the PBG structure can work similar as a metallic waveguide for modes in the gap. Compared to a DLW structure, we still need a dielectric layer for the efficient beam excitation. Further study shows that this can be achieved by adding dielectric cylinders and

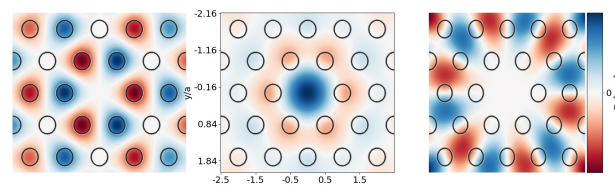


Figure 4: Three consecutive modes from three different TM bands.

the gap is tunable. We will expand these ideas with 3D simulations in a future publication.

TUNABILITY OF THE WAVEGUIDE

In order to tune the mode, there are ,broadly speaking, two approaches: 1. update of the photonic crystals by employing scale invariance of Maxwell equations; 2. change of the defects. In the first approach it requires that all the rods can be motorized so that the periodicity of the crystal can be modified mechanically. For a single mode PBG, this can essentially scan some frequency range that the user wants. Since the device is working under hundred μm range, the tuning accuracy with a small fraction of the wavelength can be guaranteed with the current techniques. For the second method, the surrounding dielectric layers are fixed, namely the basic crystal structure. The tunability lies in the change of the defect region. The first approach clearly provides higher degree of freedom but at the same time necessities also a lot of engineering efforts.

In order to test the idea experimentally, as the first step, we can create a relatively large structure in hundred GHz range without any motorization. The mechanical supports are provided at both ends of the structure. After discussion with local nano-fabrication group at PSI, this seems feasible by directly assembling the dielectric rods available from the market.

In next section, we briefly introduce the chamber at SwissFEL, which can potentially host our experiments.

ACHIP

The experiments could be performed in the experimental chamber [20] that was built in the framework of the Accelerator-on-a-Chip International Program (ACHIP) at PSI [16]. The chamber is equipped with a hexapod, which can be used to position the terahertz structure into the electron beam. Permanent magnet quadrupole triplets are installed upstream and downstream of the interaction point. These are used to match the electron beam into the structure. Each quadrupole can be positioned with micrometer accuracy. Matching of the electron beam will be performed using the electromagnetic quadrupoles before the interaction chamber.

The electron beam is derived from the SwissFEL linear accelerator. Located about 320 meters from the electron gun, the electrons have an energy of up to 3 GeV. The bunch charge can be varied between 1 and 200 pC, and the bunch

length can be adjusted to values between 10 fs and 3 ps rms. The quadrupole magnets in the interaction chamber can focus this beam into the strucutre, and the minimum focus size is expected to be smaller than 1 μm rms. Sub-micrometer wire scanners will be used to measure the beam size in the interaction region [21]. A loss monitor, consisting of a scintillating fiber that is coupled to a photo multiplier tube, can help align the electron beam w.r.t THz structure under test. The 3D engineering model is shown in Fig. 5.

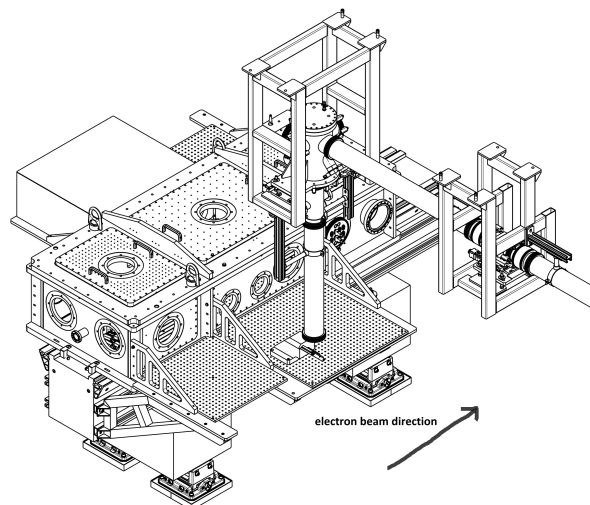


Figure 5: Experimental chamber, installed in the ATHOS beam line of SwissFEL.

CONCLUSION AND OUTLOOK

We have showed the principal study of a photonic band gap structure that can be potentially used for tunable THz generation. The band structure for TE/TM modes are presented. By removing a central rod, close to 50% of the mode energy can be trapped in the defect site. The tunability of the mode comes from either the local or global modifications of the crystal. We are also preparing for the experimental infrastructure in the synergy with ACHIP project. Motorizing the structure to obtain the full tunability still requires significant amount of engineering efforts. We in the near future plan to make a structure in the mm range.

The PBG represents a wealth of possibilities for light control in general. It is particularly interesting to us because it promises a possible solution framework for generation, coupling, filtering and transport. This will provide us a full photonic approach in THz range, e.g., the Bragg fiber for high power THz pulse transport.

ACKNOWLEDGEMENTS

We thank the discussion with the colleagues from Nanofabrication group locally at PSI. This project has received funding from the European Union's Horizon 2020 research and innovation programme under the Marie Skłodowska-Curie grant agreement No 701647.

REFERENCES

- [1] J.-M. Manceau, P. Loukakos, and S. Tzortzakis, "Direct acoustic phonon excitation by intense and ultrashort terahertz pulses," *Applied Physics Letters*, vol. 97, no. 25, p. 251 904, 2010.
- [2] S. Kovalev *et al.*, "Probing ultra-fast processes with high dynamic range at 4th-generation light sources: Arrival time and intensity binning at unprecedented repetition rates," *Structural Dynamics*, vol. 4, no. 2, p. 024 301, 2017.
- [3] C. Vicario, B. Monoszlai, C. Ruchert, and C. P. Hauri, "High-field laser-based terahertz source for SwissFEL," in *Proceedings, FEL13, New York, USA.*, 2013, pp. 438–441.
- [4] R. A. Lewis, "A review of terahertz sources," *Journal of Physics D: Applied Physics*, vol. 47, no. 37, p. 374 001, 2014.
- [5] T. Kampfrath, K. Tanaka, and K. A. Nelson, "Resonant and nonresonant control over matter and light by intense terahertz transients," *Nature Photonics*, vol. 7, no. 9, pp. 680–690, 2013, issn: 17494885. doi: 10.1038/nphoton.2013.184.
- [6] A. Altmark and A. Kanareykin, "The source of THz radiation based on dielectric waveguide excited by sequence of electron bunches," in *Journal of Physics: Conference Series*, IOP Publishing, vol. 732, 2016, p. 012 037.
- [7] S. Antipov *et al.*, "Subpicosecond bunch train production for a tunable mJ level THz source," *Physical Review Letters*, vol. 111, no. 13, p. 134 802, 2013.
- [8] S. Antipov *et al.*, "High power terahertz radiation source based on electron beam wakefields," *Review of Scientific Instruments*, vol. 84, no. 2, p. 022 706, 2013.
- [9] W. Li *et al.*, "Tunable THz radiation source from dielectric loaded waveguide excited by nonrelativistic electron bunch trains," *Phys. Rev. ST Accel. Beams*, vol. 19, p. 104 701, 10 2016. doi: 10.1103/PhysRevAccelBeams.19.104701.
- [10] C. Milne *et al.*, "SwissFEL: The Swiss X-ray Free Electron Laser," *Applied Sciences*, vol. 7, no. 7, p. 720, 2017.
- [11] J. D. Joannopoulos, S. G. Johnson, J. N. Winn, and R. D. Meade, *Photonic Crystals: Molding the Flow of Light - Second Edition*, REV - Revised, 2. Princeton University Press, 2008.
- [12] D. R. Smith, S. Schultz, N. Kroll, M. Sigalas, K. M. Ho, and C. M. Soukoulis, "Experimental and theoretical results for a two-dimensional metal photonic band-gap cavity," *Applied Physics Letters*, vol. 65, no. 5, pp. 645–647, 1994. doi: 10.1063/1.112258.
- [13] E. I. Smirnova, A. S. Kesar, I. Mastovsky, M. A. Shapiro, and R. J. Temkin, "Demonstration of a 17-GHz, high-gradient accelerator with a photonic-band-gap structure," *Physical Review Letters*, vol. 95, no. 7, p. 074 801, 2005.
- [14] E. I. Smirnova, I. Mastovsky, M. A. Shapiro, R. J. Temkin, L. M. Earley, and R. L. Edwards, "Fabrication and cold test of photonic band gap resonators and accelerator structures," *Phys. Rev. ST Accel. Beams*, vol. 8, p. 091 302, 9 2005. doi: 10.1103/PhysRevSTAB.8.091302.
- [15] P. D. Hoang *et al.*, "Experimental characterization of electron-beam-driven wakefield modes in a dielectric-woodpile cartesian symmetric structure," *Physical Review Letters*, vol. 120, p. 164 801, 16 2018. doi: 10.1103/PhysRevLett.120.164801.
- [16] E. Prat *et al.*, "Outline of a dielectric laser acceleration experiment at SwissFEL," *Nuclear Instruments and Methods in Physics Research Section A: Accelerators, Spectrometers, Detectors and Associated Equipment*, vol. 865, pp. 87–90, 2017.
- [17] T. P. Wangler, *RF Linear Accelerators*, 2nd Completely Revised and Enlarged Edition. Wiley, Weinheim, 2008.
- [18] M. Ibanescu *et al.*, "Analysis of mode structure in hollow dielectric waveguide fibers," *Phys. Rev. E*, vol. 67, p. 046 608, 4 2003. doi: 10.1103/PhysRevE.67.046608.
- [19] S. G. Johnson and J. D. Joannopoulos, "Block-iterative frequency-domain methods for Maxwell's equations in a planewave basis," *Optics express*, vol. 8, no. 3, pp. 173–190, 2001.
- [20] E. Ferrari *et al.*, "The ACHIP experimental chambers at the Paul Scherrer Institut," *Nuclear Instruments and Methods in Physics Research Section A: Accelerators, Spectrometers, Detectors and Associated Equipment*, vol. 907, pp. 244–247, 2018. doi: 10.1016/j.nima.2018.02.112.
- [21] S. Borrelli *et al.*, "Generation and measurement of sub-micrometer relativistic electron beams," *Communications Physics*, vol. 1, no. 1, p. 52, 2018. doi: 10.1038/s42005-018-0048-x.